

*DIFFERENTIAL EQUATIONS  
AND  
CONTROL PROCESSES*  
N 4, 2009

*Electronic Journal,  
reg. N P2375 at 07.03.97  
ISSN 1817-2172*

*<http://www.neva.ru/journal>  
<http://www.math.spbu.ru/diffjournal/>  
e-mail: [jodiff@mail.ru](mailto:jodiff@mail.ru)*

## **Transient Natural Convection near a Semi-Infinite Vertical Wall in a Rotating System**

**Pallath Chandran**

Department of Mathematics and Statistics  
College of Science, Sultan Qaboos University  
PC 123, Al Khod, Muscat, Sultanate of Oman  
E-mail: [chandran@squ.edu.om](mailto:chandran@squ.edu.om)

**Nirmal C Sacheti**

Department of Mathematics and Statistics  
College of Science, Sultan Qaboos University  
PC 123, Al Khod, Muscat, Sultanate of Oman  
E-mail: [nirmal@squ.edu.om](mailto:nirmal@squ.edu.om)

**Ashok K. Singh**

Department of Mathematics, Faculty of Science  
Banaras Hindu University  
Varanasi – 221005, India  
E-mail: [ashok@bhu.ac.in](mailto:ashok@bhu.ac.in)

### **Abstract**

The natural convection in an incompressible viscous fluid flowing near a semi-infinite impermeable vertical plate has been investigated. Assuming that the fluid-plate system is undergoing a rigid-body rotation, the nonlinear set of governing boundary layer momentum and thermal equations has been solved using an appropriate implicit finite difference numerical scheme. The effect of the rotation parameter on the developing flow has been discussed in detail for

a specific fluid. Shear stress and heat transfer parameters have also been computed and analysed.

## 1 Introduction

Investigation of the natural convection transport processes involving the coupling of the fluid flow and heat transfer has attracted the attention of several researchers because of its varied applications in many engineering fields and naturally occurring systems. Rotation effects on natural convection flows are important in many engineering applications such as nuclear power plants, cooling of nuclear reactors and electronic systems, atmospheric re-entry of space vehicles, gas turbines, spin-stabilised missiles and various propulsion devices for missiles, satellites and space vehicles. Natural convection in a rotating system also finds applications in petroleum engineering for observing the movement of oil and gas through a reservoir. Among the theoretical studies related to natural convection in viscous incompressible fluids, the convection taking place near vertical plates — both of infinite as well as semi-infinite extent — has been extensively dealt with in literature. Most of these studies have focused on flow near an infinite plate or between two vertical walls. However, when the convection takes place near a semi-infinite vertical plate, the analysis of the governing fluid dynamical equations becomes more challenging, generally requiring numerical treatment.

Steady free convection flow of a viscous incompressible fluid past a semi-infinite vertical wall was first discussed by Pohlhausen [1] using an integral method. Decades later, Ostrach [2] studied the same problem by obtaining similarity solutions of the governing equations. Unsteady free convective motion of a viscous incompressible fluid bounded by a semi-infinite vertical wall has been presented by Siegel [3] and Gebhart [4] by incorporating the integral and approximation methods, respectively. Mass transfer effects on the developing free convective flow past a semi-infinite flat plate has been investigated by Callahan and Marner [5] using an explicit finite difference method. This problem has also been analysed by Soundalgekar and Ganesan [6] using an implicit finite difference method. These authors have demonstrated that the two methods yield comparable results. Raptis *et al.* [7] have presented numerical solution of transient free convective flow in a porous medium bounded by a semi-infinite vertical plate. They used an explicit finite difference algorithm. Singh and Rai [8] solved the governing equations of free convective flow of water at 4° C past a

semi-infinite vertical plate. Free convection heat transfer near the leading edge of an isothermal semi-infinite vertical flat plate with finite thickness has been investigated numerically by Miyamoto and Akiyoshi [9]. The effect of variable surface temperature on the free convection in a viscous fluid past a semi-infinite plate has been discussed by Takhar *et al.* [10]. Recently, the present authors [11, 12] considered the effect of temporally ramped temperature distribution on free convection under the same geometrical configuration, and brought out certain features of the flow for a range of values of Prandtl number.

In the present work, we consider transient free convective flow of a viscous incompressible fluid past a semi-infinite vertical wall. It is assumed that the convection is set up by a change in the temperature of the wall from that of the fluid temperature. The main thrust of this study is to analyse the effect of rigid body rotation of the plate-fluid system. The problem — formulated in terms of a nonlinear initial-boundary-value problem — has been solved numerically using an implicit finite difference method of Crank-Nicolson type.

## 2 Governing equations

The geometrical configuration of the fluid-plate system comprises a semi-infinite vertical wall bounding an infinite expanse of the fluid. The  $x'$ -axis of the co-ordinate system  $Ox'y'z'$  is taken along the vertical wall in the upward direction,  $y'$ -axis along the wall in horizontal direction and  $z'$ -axis perpendicular to the wall but into the fluid. The origin of the co-ordinate system is at the lower end of the wall. Initially the temperatures of the fluid as well as the wall are constant, denoted by  $T'_\infty$ . At time  $t' > 0$ , the temperature of the wall,  $z' = 0$ , is instantaneously raised or lowered to  $T'_w$  and thereafter maintained at the same temperature. The whole system is assumed to be rotating with a constant angular velocity  $\Omega'$  about the  $z'$ -axis. Also, it is assumed that all the fluid properties are constant except that the influence of the density variation with temperature is included in the body force term. Under the usual Boussenesq approximation, the governing conservation equations for the continuity, momentum and energy, near the vertical plate, can be obtained from Ker and Lin [13] in the form

$$\frac{\partial u'}{\partial x'} + \frac{\partial w'}{\partial z'} = 0 \quad (1)$$

$$\frac{\partial u'}{\partial t'} + u' \frac{\partial u'}{\partial x'} + w' \frac{\partial u'}{\partial z'} - 2\Omega' v' = \nu \frac{\partial^2 u'}{\partial z'^2} + g\beta(T' - T'_\infty) \cos(\Omega' t') \quad (2)$$

$$\frac{\partial v'}{\partial t'} + u' \frac{\partial v'}{\partial x'} + w' \frac{\partial v'}{\partial z'} + 2\Omega' u' = \nu \frac{\partial^2 v'}{\partial z'^2} - g\beta(T' - T'_\infty) \sin(\Omega' t') \quad (3)$$

$$\frac{\partial T'}{\partial t'} + u' \frac{\partial T'}{\partial x'} + w' \frac{\partial T'}{\partial z'} = \frac{\kappa}{\rho C_p} \frac{\partial^2 T'}{\partial z'^2} \quad (4)$$

with the initial and boundary conditions

$$t' \leq 0 : u' = 0, v' = 0, w' = 0, T' = T'_\infty, \text{ for } 0 \leq x', z' < \infty$$

$$t' > 0 : \begin{cases} u' = 0, v' = 0, w' = 0, T' = T'_\infty, & \text{at } x' = 0 \\ u' = 0, v' = 0, w' = 0, T' = T'_w, & \text{at } z' = 0 \\ u' \rightarrow 0, v' \rightarrow 0, T' \rightarrow T'_\infty, & \text{as } z' \rightarrow \infty \end{cases} \quad (5)$$

The symbols used above and to follow later, have been defined in the **Nomenclature**, at the end. Introducing the non-dimensional variables

$$(x, z) = (x', z')/L, \quad t = \nu t'/L^2, \quad \Omega = L^2 \Omega'/\nu, \quad (6)$$

$$(u, v, w) = (u' v' w')L/\nu, \quad T = (T' - T'_\infty)/(T'_w - T'_\infty),$$

equations (1)–(4) become

$$\frac{\partial u}{\partial x} + \frac{\partial w}{\partial z} = 0 \quad (7)$$

$$\frac{\partial u}{\partial t} + u \frac{\partial u}{\partial x} + w \frac{\partial u}{\partial z} - 2\Omega v = \frac{\partial^2 u}{\partial z^2} + T \cos(\Omega t) \quad (8)$$

$$\frac{\partial v}{\partial t} + u \frac{\partial v}{\partial x} + w \frac{\partial v}{\partial z} + 2\Omega u = \frac{\partial^2 v}{\partial z^2} - T \sin(\Omega t) \quad (9)$$

$$\frac{\partial T}{\partial t} + u \frac{\partial T}{\partial x} + w \frac{\partial T}{\partial z} = \frac{1}{\text{Pr}} \frac{\partial^2 T}{\partial z^2} \quad (10)$$

In the above non-dimensionalisation process, we have employed a characteristic length  $L$  defined by

$$L = \left( \frac{\nu^2}{g\beta(T'_w - T'_\infty)} \right)^{1/3} \quad (11)$$

The non-dimensional parameter  $\text{Pr}$  ( $= C_p \mu / \kappa$ ) appearing in equation (10), is the well-known Prandtl number. The initial and boundary conditions for the velocity and temperature fields given by equation (5) can be expressed in non-dimensional form as

$$t \leq 0 : u = 0, v = 0, w = 0, T = 0 \text{ for } 0 \leq x, z < \infty$$

$$t > 0 : \begin{cases} u = 0, v = 0, w = 0, T = 0, & \text{at } x = 0 \\ u = 0, v = 0, w = 0, T = 1, & \text{at } z = 0 \\ u \rightarrow 0, v \rightarrow 0, T \rightarrow 0, & \text{as } z \rightarrow \infty \end{cases} \quad (12)$$

### 3 Numerical solution procedure

The non-linearity of the partial differential equations governing the flow suggests that solutions of the equations must be sought numerically. The simultaneous non-linear partial differential equations (7)–(10) with conditions (12) are to be solved for the dependent variables  $u$ ,  $v$ ,  $w$ ,  $T$  as functions of  $x$ ,  $z$  and  $t$ . Of particular interest is also the steady state solution if it exists. We use here the implicit finite difference method of Crank-Nicolson type for the numerical solution. The finite difference equations corresponding to equations (8)–(10) are transformed into a system of equations in tridiagonal form after some algebraic manipulations and, then, they are solved by the Thomas algorithm.

The space under consideration has been restricted to finite dimensions. Here a plate of height  $x_{\max} = 20$  and  $z_{\max} = 20$  have been considered. As the large number of grid points yield a better estimate of the dependent variables, we have taken a grid of size  $201 \times 201$  to evaluate the variables. Computations have been carried out for a fluid of Prandtl number 0.71 (which corresponds to air). During any one time step, the computed values of the previous time step have been used for the coefficients  $u$  and  $w$  appearing in the equations (8)–(10).

At the end of each time step, first the temperature field has been obtained and then the evaluated values are employed to obtain the velocity components in  $x$ - and  $y$ -directions. Finally, velocity component  $w$  in the  $z$ -direction is obtained using equation (7). Unsteady values of the velocity and temperature fields corresponding to a particular time have been reported when the time is achieved by iterative process. The process of computation is advanced until a steady state is approached with respect to the temperature and velocity fields by satisfying the convergence criterion

$$\sum_i \sum_j |A_{i,j}^{k+1} - A_{i,j}^k| < 10^{-5} \sum_i \sum_j |A_{i,j}^{k+1}| \quad (13)$$

where  $A_{i,j}^k$  stands for the velocity or temperature field.

In the numerical computation, special attention is required to specify  $\Delta t$  in order to get a steady state solution as soon as possible, yet small enough to avoid instabilities. We set  $\Delta t$  as

$$\Delta t = \lambda \times \min(\Delta x^2, \Delta z^2) \quad (14)$$

where  $\Delta x$  and  $\Delta z$  are mesh sizes along the  $x$  and  $z$  directions, respectively. The stabiliser parameter  $\lambda$  is guessed by numerical experimentations in order

to achieve convergence and stability of the solution procedure. A series of numerical experiments has shown that assigning the value 2 to  $\lambda$  is suitable for numerical computations.

It is worth mentioning here that the numerical procedure used herein has been seen to be quite satisfactory as far as its accuracy is concerned. To see the accuracy and convergence of the results, the program was re-run by refining the grid system as well as the time step. For instance, when the program was run with the  $251 \times 251$  grid size with a smaller time step than used before, no significant changes in the results were observed. Moreover, we were also able to validate the numerical results for the special case when rotation was absent.

Having solved for the velocity and temperature variables, one can compute the shear stress and heat transfer parameters at the vertical wall. The local skin friction components in the  $x$  and  $y$  directions — denoted by  $\tau_x$  and  $\tau_y$  — are defined as

$$\tau_x = \frac{L^2 \tau_{x'}}{\rho \nu^2} = \frac{\partial u}{\partial z} \Big|_{z=0}, \quad \tau_y = \frac{L^2 \tau_{y'}}{\rho \nu^2} = - \frac{\partial v}{\partial z} \Big|_{z=0} \quad (15)$$

The average values of the skin friction components with respect to the variable  $x$  are given by

$$\tau_{xav} = \frac{1}{x_{\max}} \int_0^{x_{\max}} \tau_x dx, \quad \tau_{yav} = \frac{1}{x_{\max}} \int_0^{x_{\max}} \tau_y dx \quad (16)$$

The quantities  $\tau_x$  and  $\tau_y$  have been evaluated using a five-point forward finite difference formula for first derivative, and then  $\tau_{xav}$  and  $\tau_{yav}$  have been computed using the Simpson's rule. In a similar way, the Nusselt number  $Nu$  and average Nusselt number  $Nu_{av}$  have been computed from the temperature field variable using the formulae

$$Nu = \frac{qL}{\kappa(T'_w - T'_\infty)} = - \frac{\partial T}{\partial z} \Big|_{z=0}, \quad Nu_{av} = \frac{1}{x_{\max}} \int_0^{x_{\max}} Nu dx \quad (17)$$

## 4 Results

Our main focus in this work is to determine the influence of the rigid body rotation on the developing fluid motion. To this end, we have computed and shown the effects of rotation parameter  $\Omega$  and the non-dimensional time variable  $t$  on various physical quantities of interest.

In Figs 1–3, we have presented the plots of velocity components  $u$ ,  $v$ ,  $w$  versus  $z$  at a cross-section  $x = \text{const}$ . In these plots, the effects of  $t$  and  $\Omega$  on the

velocity components have been shown in detail. From Fig 1, we observe that the velocity component  $u$  increases near the vertical plate, attains a maximum, and then decreases to its free-stream value in conformity with the boundary layer feature. We further notice that  $\Omega$  has a retarding effect on  $u$  for a fixed  $t$ . However, as  $t$  increases, the effect of  $\Omega$  on  $u$  becomes more pronounced. It may also be noted that the peaks of these velocity curves shift progressively away from the bounding wall as  $t$  increases. The behaviour of the  $y$ -component  $v$  of velocity at the cross-section  $x = 10$ , is shown in Fig 2. The magnitude of  $v$  increases with  $\Omega$  for a fixed value of  $t$ . The behaviour of  $|v|$  with  $t$  is similar to that observed for the  $u$ -profiles. In Fig 3, we have shown profiles for the normal velocity component  $w$  at the cross-section  $x = 5$ . Due to the rotation of the bounding vertical plate, the fluid is drawn towards it. The effect of rotation is to enhance the magnitude of  $w$ , similar to that noticed for  $v$ .

As stated before, our main aim in this work has been to investigate the effect of rigid body rotation on the natural convection near the semi-infinite vertical plate. When rotation is absent ( $\Omega = 0$ ), the secondary velocity  $v$  should vanish for all values of  $t$ . This has further been confirmed from the numerical solution of the system of equations (7)–(10) in conjunction with equation (12). It was seen that for this case,  $v$  becomes zero for all  $t$ . The values of the other velocity components  $u$  and  $w$  undergo some variations when rotation is absent. For illustrative purpose, we have shown in Fig (1a) the variation of the velocity component  $u$  corresponding to  $\Omega = 0$ . The velocity profiles  $u$  for this particular case are in agreement with an earlier study reported in literature [14]. The profiles of  $u$  for the non-rotating and rotating cases are qualitatively very similar, as can be seen from Figs 1 and (1a). However, the presence of rotation tends to diminish the velocity, in agreement with our earlier observation.

In Fig 4, we have shown variation of the temperature of the fluid for a set of values of  $\Omega$  and  $t$  — similar to the ones used in Figs 1–3. For a fixed value of the parameter  $t$ , the effect of increase of rotation parameter is to enhance the temperature in the boundary layer region. A similar behaviour is also observed for the temperature when  $\Omega$  is fixed and  $t$  increases. As a consequence, the thermal boundary layer thickness increases proportionate to both  $\Omega$  and  $t$ . In Figs 5 and 6, we have plotted a number of isotherms ( $T = \text{const.}$  curves) in the  $xz$ -plane corresponding to  $\Omega = 0.05$  and  $0.1$ , respectively. Each of these figures includes the constant temperature profiles for four different temporal situations. It is to be noted that the increase in the thermal boundary layer thickness, stated earlier, is yet again conspicuous in the set of figures 5–6.

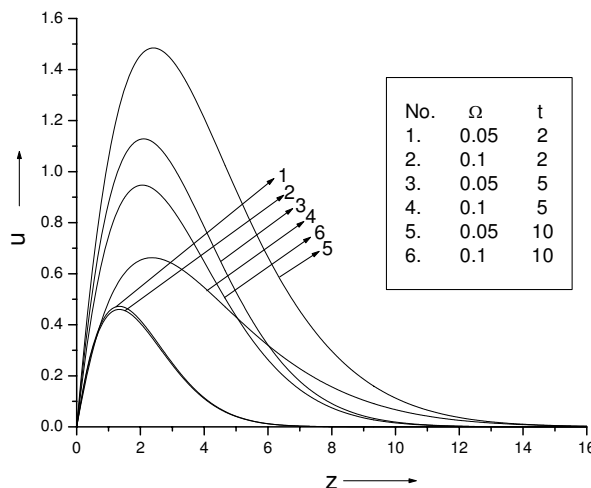


Fig 1. Profiles of velocity  $u$  at  $x = 10$  for different values of  $t$  and  $\Omega$

The shear stress and heat transfer on the bounding plate play important roles in the design processes in several engineering and industrial applications. Thus, the variation of these quantities has been exhibited in Figs 7–9. It may be noted that increasing the rotation results in the desired reduction in the  $x$ -component of the shear stress  $\tau_x$  (Fig 7) for a given value of  $t$ . However, such a monotonic behaviour is not observed with respect to the temporal parameter for a fixed value of  $\Omega$ . On the other hand,  $|\tau_y|$  behaves monotonically with respect to both  $\Omega$  and  $t$ , as can be seen from Fig 8. In the last Fig 9, we have shown the plot of the Nusselt number  $Nu$  with  $x$  for a combination of values of  $t$  and  $\Omega$ . It is seen that near the leading edge,  $Nu$  drops appreciably. Furthermore, both parameters  $\Omega$  and  $t$  have a diminishing effect on this heat

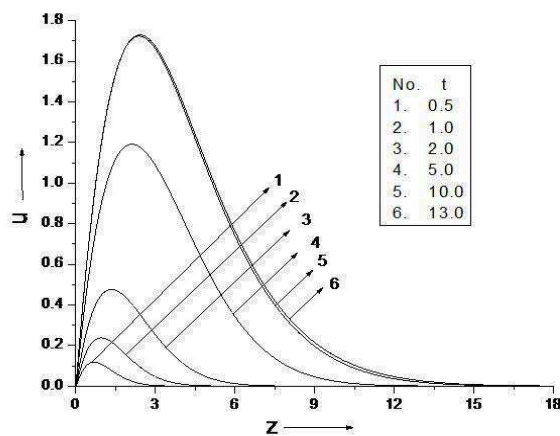


Fig 1a. Profiles of velocity  $u$  at  $x = 10$  for different values of  $t$ . ( $\Omega = 0$ )

transfer parameter.

Finally, we have given in Table 1 the computed average values of the skin-friction components and the Nusselt number. For the range of parameter values considered in this analysis, the following observations are worth noting:

- For a fixed value of  $t$ , the average values of all three quantities  $\tau_{xav}$ ,  $\tau_{yav}$  and  $Nu_{av}$  show monotonic behaviour although the variations are more noticeable for large values of  $t$ .
- Both  $\tau_{xav}$  and  $Nu_{av}$  decrease while  $\tau_{yav}$  increases with  $\Omega$  — in conformity with their local counterparts.
- Both shear stress averages increase with  $t$  for a fixed value of rotation

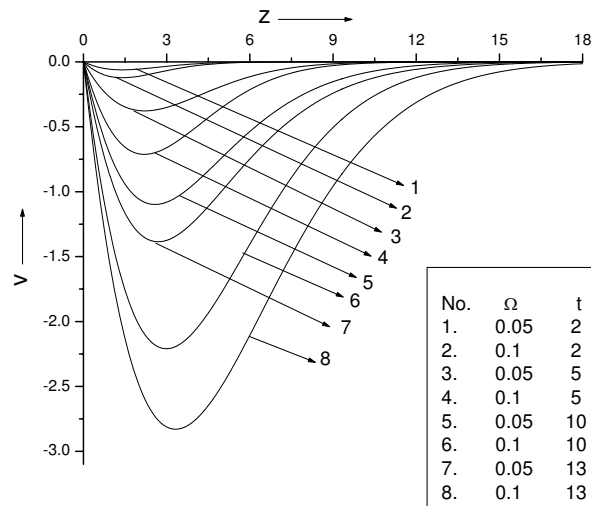


Fig 2. Profiles of velocity  $v$  at  $x = 10$  for different values of  $t$  and  $\Omega$

parameter while the opposite occurs for the quantity  $Nu_{av}$ .

## Nomenclature

- $c_p$  specific heat at constant pressure  
 $g$  acceleration due to gravity  
 $L$  characteristic length (defined in equation (11))  
 $Nu$  Nusselt number at the bounding wall  
 $Nu_{av}$  average Nusselt number at the wall  
 $Pr$  Prandtl number  
 $q$  rate of heat transfer

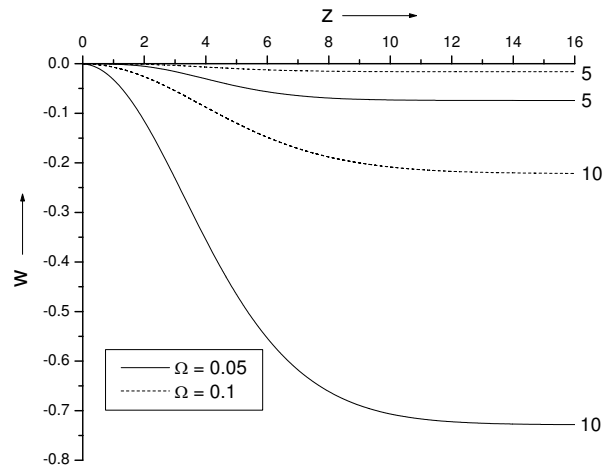


Fig 3. Profiles of velocity  $w$  at  $x = 5$  for different values of  $t$  and  $\Omega$

- $t'$  time
- $t$  time in non-dimensional form
- $T'$  temperature of the fluid
- $T$  non-dimensional temperature
- $T'_\infty$  initial temperature of the fluid and wall
- $T'_w$  temperature of the wall for  $t > 0$
- $u'$  velocity component of the fluid in the  $x'$ -direction
- $u$  non-dimensional form of  $u'$
- $v'$  velocity of the fluid in the  $y'$ -direction
- $v$  non-dimensional form of  $v'$
- $w'$  velocity of the fluid in the  $z'$ -direction

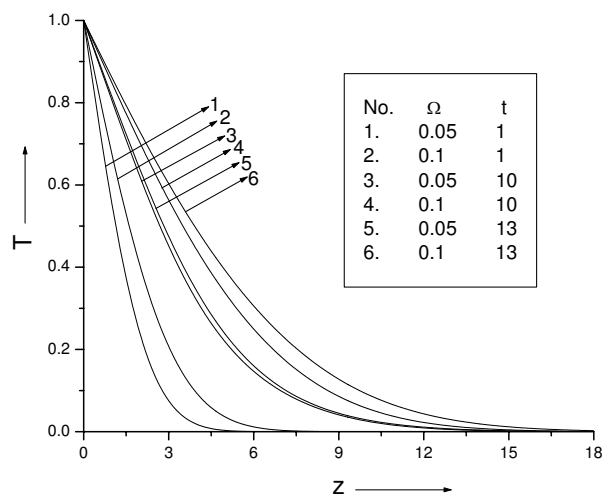


Fig 4. Profiles of temperature T at  $x = 10$  for different values of t and  $\Omega$

- $w$  non-dimensional form of  $w'$
- $x'$  space coordinate along the wall
- $x$  dimensionless form of  $x'$
- $z'$  space coordinate perpendicular to the wall
- $z$  dimensionless form of  $z'$

### Greek symbols

- $\beta$  coefficient of thermal expansion
- $\mu$  dynamic viscosity of the fluid
- $\nu$  kinematic viscosity of the fluid

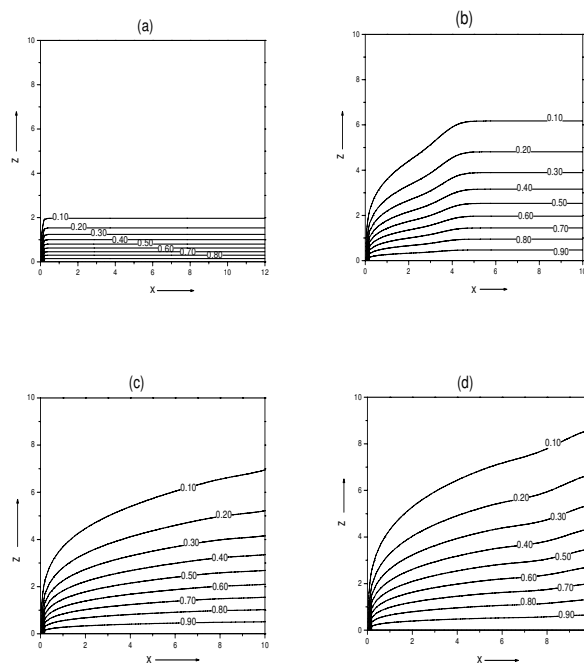


Fig 5. Isotherms for  $\Omega = 0.05$

(a)  $t = 1$  (b)  $t = 5$  (c)  $t = 10$  (d)  $t = 13$

- $\kappa$  thermal conductivity of the fluid
- $\tau_{x'}$  skin-friction at the wall in the  $x'$ -direction
- $\tau_x$  non-dimensional skin friction in the  $x$ -direction
- $\tau_{xav}$  average skin-friction at the wall in the  $x$ -direction
- $\tau_{y'}$  skin-friction at the wall in the  $y'$ -direction
- $\tau_y$  non-dimensional skin friction in the  $y$ -direction
- $\tau_{yav}$  average skin-friction at the wall in the  $y$ -direction
- $\Omega'$  angular velocity of the system about the  $z'$ -axis
- $\Omega$  Non-dimensional form of  $\Omega'$

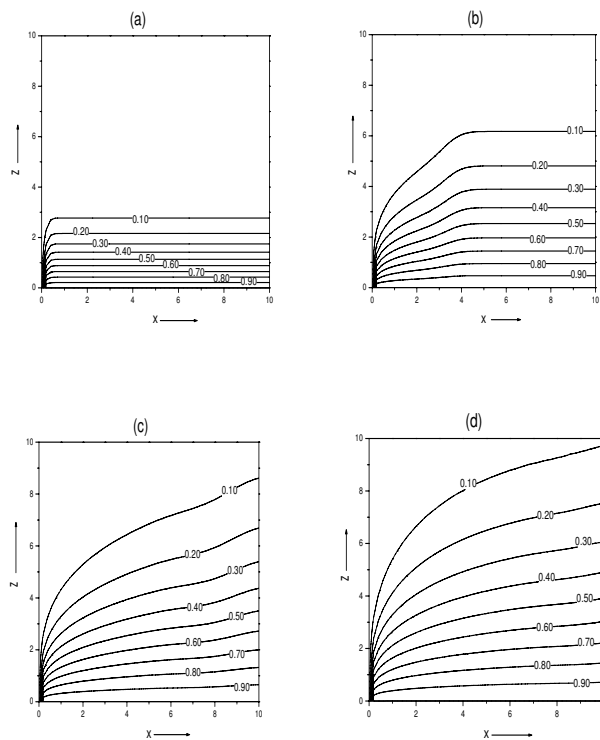


Fig 6. Isotherms for  $\Omega = 0.1$

(a)  $t = 1$  (b)  $t = 5$  (c)  $t = 10$  (d)  $t = 13$

## References

- [1] E. Pohlhausen: Der Warenaustausch zwischen festen Körpern und Flüssigkeiten mit kleiner Reibung und Kleinerwärmeleitung, *Z. Angew. Math. Mech.*, **1** (1921) 115.
- [2] S. Ostrach: An analysis of laminar free convection flow heat transfer about a flat plate parallel to the direction of the generating body force, NASA Report No. 1111 (1953).
- [3] R. Siegel: Transient free convection from a vertical flat plate, *Trans. Amer. Soc. Mech. Eng.*, **80** (1958) 347.

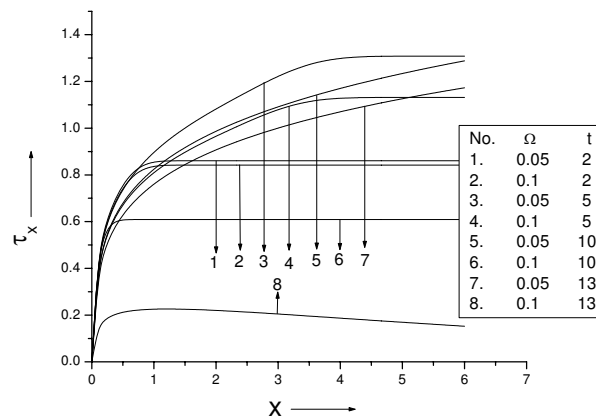


Fig 7. Variation of local skin friction component  $\tau_x$  for different t and  $\Omega$

- [4] B. Gebhart: Transient natural convection from vertical elements, *J. Heat Transfer*, **83C** (1961) 61.
- [5] G. D. Callahan and W. J. Marner: Transient free convection with mass transfer on an isothermal vertical flat plate, *Int. J. Heat and Mass Transfer*, **19** (1976) 165.
- [6] V. M. Soundalgekar and P. Ganesan: Transient free convective flow past a semi-infinite vertical plate with mass transfer, *Reg. J. Energy Heat Mass Transfer*, **2** (1980) 83.
- [7] A. Raptis, A. K. Singh and K. D. Rai: Finite difference analysis of unsteady free convective flow through a porous medium adjacent to a semi-infinite

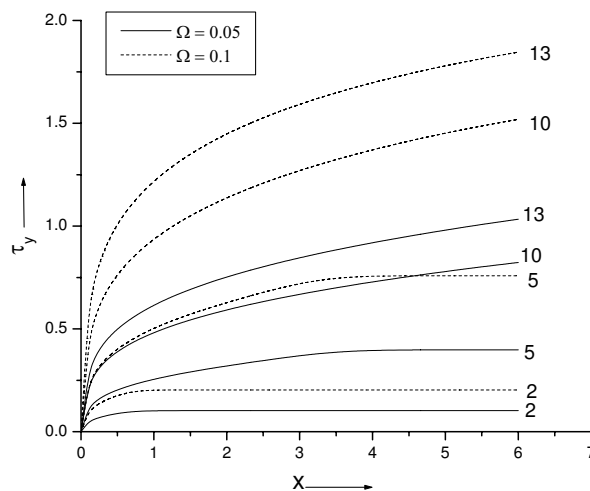


Fig 8. Variation of local skin friction component  $\tau_y$  for different  $t$  and  $\Omega$

vertical plate, *Mech. Res. Comm.*, **14** (1987) 9.

- [8] A. K. Singh and K. D. Rai: Unsteady free convective flow of water at  $4^\circ\text{C}$  past a semi-infinite vertical plate by finite difference method, *Model. Simul. Control B*, **12** (1987) 9.
- [9] M. Miyamoto and T. Akiyoshi: Free convection heat transfer near leading edge of semi-infinite vertical flat plate with finite thickness, *Bull. Jap. Soc. Mech. Engrs. (JSME)*, **24** (1981) 1945.
- [10] H. S. Thakhar, P. Ganesan, K. Ekambavanan and V. M. Soundalgekar: Transient free convection past a semi-infinite vertical plate with variable surface temperature, *Int. J. Numer. Meth. Heat Fluid Flow*, **7** (1997) 280.

Table 1: Computed values of  $\tau_{xav}$ ,  $\tau_{yav}$  and  $Nu_{av}$ 

$\Omega$	$t$	$\tau_{xav}$	$\tau_{yav}$	$Nu_{av}$
0.05	0.5	0.432757	0.012970	0.670241
	1.0	0.608097	0.036200	0.479573
	2.0	0.846348	0.100639	0.349103
	5.0	1.213846	0.366043	0.255432
	10.0	1.226788	0.784113	0.250439
	13.0	1.110116	0.978816	0.243702
0.10	0.5	0.432161	0.025927	0.670234
	1.0	0.604791	0.072261	0.479551
	2.0	0.828177	0.199769	0.348904
	5.0	1.058542	0.702454	0.251416
	10.0	0.645576	1.441580	0.212952
	13.0	0.151594	1.752780	0.179530

- [11] A. K. Singh, E. A. Hamza, P. Chandran and N. C. Sacheti: Numerical solution of buoyancy driven unsteady flow past a semi-infinite heated vertical plate with ramped temperature distribution, *Proc. Conference on Mathematics and its Applications*, The University of West Indies, Trinidad (2006).
- [12] A. K. Singh, N. C. Sacheti and P. Chandran: Developing flow near a semi-infinite vertical wall with ramped temperature, *Int. J. Appl. Math. Stat.*, **13** (2008) 34.
- [13] Y. T. Ker and T. F. Lin: A combined numerical and experimental study of air convection in a differentially heated rotating cubic cavity, *Int. J. Heat Mass Transfer*, **39** (1996) 3193.
- [14] B. Carnahan, H. A. Luther and J. O. Wilkes: *Applied Numerical Methods*, John Wiley, New York (1969).

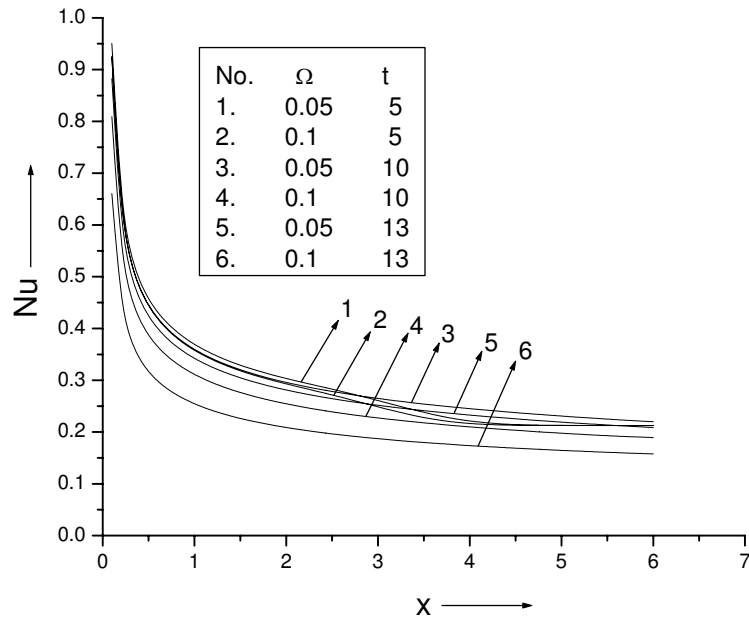


Fig 9. Variation of Nusselt number Nu for different t and  $\Omega$